Bose-Einstein Condensation of $S = 1$ Nickel Spin Degrees of Freedom in $NiCl_2$-4SC$(NH_2)_2$

V. S. Zapf,[1] D. Zocco,[1] B. R. Hansen,[2,3] M. Jaime,[1] N. Harrison,[1] C. D. Batista,[4] M. Kenzelmann,[2,3] C. Niedermayer,[3] A. Lacerda,[1] and A. Paduan-Filho[5]

[1]*National High Magnetic Field Laboratory, Los Alamos, New Mexico, USA*
[2]*Laboratory for Solid State Physics, ETH Hönggerberg, CH-8093 Zürich, Switzerland*
[3]*Laboratory for Neutron Scattering, ETH Zürich and Paul Scherrer Institute, CH-5232 Villigen, Switzerland*
[4]*Condensed Matter and Statistical Physics, Los Alamos National Laboratory, Los Alamos, New Mexico, USA*
[5]*Instituto de Fisica, Universidade de Sao Paulo, Sao Paulo, Brazil*

(Received 20 May 2005; published 23 February 2006)

It has recently been suggested that the organic compound $NiCl_2$-4SC$(NH_2)_2$ (DTN) undergoes field-induced Bose-Einstein condensation (BEC) of the Ni spin degrees of freedom. The Ni $S = 1$ spins exhibit three-dimensional XY antiferromagnetism above a critical field $H_{c1} \sim 2$ T. The spin fluid can be described as a gas of hard-core bosons where the field-induced antiferromagnetic transition corresponds to Bose-Einstein condensation. We have determined the spin Hamiltonian of DTN using inelastic neutron diffraction measurements, and we have studied the high-field phase diagram by means of specific heat and magnetocaloric effect measurements. Our results show that the field-temperature phase boundary approaches a power-law $H - H_{c1} \propto T_c^{\alpha}$ near the quantum critical point, with an exponent that is consistent with the 3D BEC universal value of $\alpha = 1.5$.

DOI: 10.1103/PhysRevLett.96.077204 PACS numbers: 75.40.−s, 65.40.Ba

In the past few years, quantum spin systems exhibiting magnetic-field-induced quantum phase transitions (QPT) to an antiferromagnetic (AF) phase have received an increasing amount of attention. The compounds studied to date consist of weakly coupled chains of $S = 1$ Ni atoms [1–3], planes of Cu dimers, ($BaCuSi_2O_6$) [4,5], or 3D coupled spin ladders ($TlCuCl_3$ and $KCuCl_3$) [6,7]. The spin singlet ground state of these systems is separated from the lowest excited triplet state by a finite energy gap. In the presence of a magnetic field, the Zeeman term reduces the energy of the $S^z = 1$ triplet, until it reaches H_{c1}. A canted XY AF phase is then observed between H_{c1} and an upper critical field H_{c2}.

Naturally, for $H_{c1} < H < H_{c2}$, the system also undergoes a thermodynamic phase transition (TPT) at a critical temperature $T_c(H)$. However, the thermodynamic and quantum phase transitions are qualitatively different. In the TPT, the ordering is suppressed by *phase fluctuations* of the order parameter, and the corresponding critical point belongs to the $d = 3$ XY universality class. In contrast, for the field-induced QPT, the magnetic ordering is suppressed by reducing the *amplitude* of the order parameter, and the corresponding quantum critical point (QCP) belongs to the universality class of the dilute Bose gas, with an effective dimensionality $d + z$ ($z = 2$ is the dynamical exponent) [8]. The Bose gas picture is a more intuitive approach to understanding the physics of the QPT, in which each $S^z = 1$ triplet is treated as a hard-core boson. The applied field then acts like a chemical potential and the Bose gas of triplets is populated only above the critical value H_{c1}. For any finite concentration of particles $[0 < \rho < 1]$, the bosons form a Bose-Einstein condensation (BEC) that corresponds to the XY AF ordering in the original spin language.

The BEC QPT requires the spin environment to be axially symmetric with respect to the applied field. A direct consequence of this symmetry is the existence of a gapless Goldstone mode (magnons) in the ordered phase. Inelastic neutron scattering measurements were proposed to be consistent with the presence of this Goldstone mode in the ordered phase of $TlCuCl_3$ [6]. However, ESR measurements subsequently revealed a significant degree of deviation from axial symmetry [9].

The compound $NiCl_2$-4SC$(NH_2)_2$ (DTN) [10] is a new candidate for Bose-Einstein condensation of spins [11,12] and has several features that make it unique among the class of similar systems. Its tetragonal crystal structure satisfies the axial spin symmetry requirement for a BEC, and the symmetry of the spin Hamiltonian can be tuned by changing the angle between the applied field and the c axis. It has been predicted [13] that XY AF ordering should occur for fields along the c axis and Ising-like AF ordering for finite angles up to 40° away from the c axis. The single ion anisotropy $D \sim 8$ K [13,14] splits the Ni $S = 1$ spin state into the $S_z = 0$ ground state and the $S_z = \pm 1$ excited states. Thus, for $H \parallel c$, the level crossing occurs between two triplet states rather than the triplet and the singlet of the spin dimer systems. Magnetization measurements [10] have revealed AF order between $H_{c1} \sim 2$ T and $H_{c2} \sim 12$ T with a maximum Néel temperature of 1.2 K. For $H \perp c$, no transition is observed up to $H = 15$ T, since the field mixes the $S_z = 0$ state with a linear combination of the $S_z = \pm 1$ states, producing an effective repulsion between energy levels that precludes any field-induced QPT [13].

A key prediction of the BEC theory is a power-law temperature dependence of the phase transition line $H - H_{c1} \propto T_c^{\alpha}$, where $\alpha = 1.5$ for a 3D BEC [12,15,16].

Previous studies on DTN and other candidate BEC spin systems have found a wide variety of values of α higher than the predicted value of 1.5. In general, this is because the fits were performed at relatively high temperatures, whereas the power-law universal behavior is valid only for $T_c \rightarrow 0$ [5]. Furthermore, the value of α is very sensitive to the value of H_{c1} chosen for the fit, which is difficult to extrapolate from higher temperature data. A previous work found $\alpha = 2.6$ from fits to magnetization data on DTN with most of the data lying between 0.5 and 1.2 K [10]. In this present study, we obtain α from specific heat and magnetocaloric effect measurements to dilution refrigerator temperatures using an extrapolation method to zero temperature introduced by Sebastian *et al.* [5]. We are able to determine α to sufficient accuracy to rule out a 2D BEC ($\alpha = 1$) or an Ising magnet ($\alpha = 2$).

We first describe the quantitative determination of the spin Hamiltonian using neutron scattering, which is important for a microscopic understanding of the ground state and its field dependence. Zero-field neutron measurements of the low-energy magnetic excitations were performed using the cold neutron triple-axis spectrometer RITA II at the spallation neutron source SINQ at the Paul Scherrer Institute, Switzerland. The instrument was operated with a fixed final energy $E_f = 3.7$ meV, obtained with a three-blade focusing pyrolithic graphite analyzer and 80′ collimation before the sample. A cooled BeO filter with a built-in radial collimator of 80′ was placed between sample and analyzer to eliminate scattered neutrons with energies greater than 3.7 meV. Using an Oxford Instruments dilution insert in a VARIOX cryostat, a sample of three co-aligned deuterated single crystals of DTN with a combined mass of 3 g were cooled to $T = 80$ mK. The single crystals were mounted with the (hhl) crystallographic plane in the horizontal scattering plane.

Neutron scattering measurements at constant wave vector $\mathbf{Q}$ as a function of energy reveal a single magnetic peak for energy transfers below 1.1 meV after subtraction of the scattering at $T = 25$ K, as shown in Fig. 1(d). The dispersion of the magnetic excitations at zero field was determined through a series of constant-$\mathbf{Q}$ scans with $\mathbf{Q}$ along high symmetry directions in reciprocal space. The spin lattice provided by the $S = 1$ Ni ions is described by the Hamiltonian:

$$\mathcal{H} = \sum_{\mathbf{j},\nu} J_\nu \mathbf{S}_\mathbf{j} \cdot \mathbf{S}_{\mathbf{j}+\mathbf{e}_\nu} + D \sum_\mathbf{j} (S^z_\mathbf{j})^2, \tag{1}$$

where $\nu = \{a, b, c\}$ and $J_a = J_b$ due to the tetragonal symmetry of the lattice. The data were analyzed using a single-mode cross section with a dispersion obtained from a generalized spin-wave approach [13] for the disordered phase:

$$\hbar\,\omega^{\pm}_\mathbf{k} = \sqrt{\mu^2 + 2s^2\mu\gamma_\mathbf{k}} \pm g_c \mu_B H, \tag{2}$$

with

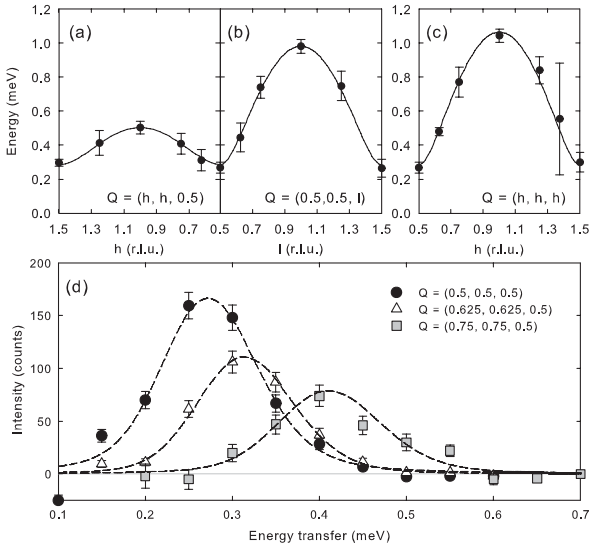

FIG. 1. (a)–(c) Dispersion of the magnetic excitations at $T = 80$ mK along three crystallographic directions. The solid line is a fit to the data using Eq. (2). (d) Background subtracted scans for the $\mathbf{Q} = (h, h, 0.5)$ direction in reciprocal space. The dashed line is a fit to a single-mode cross section as described in the text.

$$D = \mu\left[1 + \frac{1}{(2\pi)^3}\int_{-\pi}^{\pi} \frac{\gamma_\mathbf{k} d^3k}{\hbar\omega_\mathbf{k}}\right],$$
$$s^2 = 1 - \langle (S^z_\mathbf{i})^2 \rangle = 2 - \frac{1}{(2\pi)^3}\int_{-\pi}^{\pi} \frac{(\mu + s^2\gamma_\mathbf{k}) d^3k}{\hbar\omega_\mathbf{k}}, \tag{3}$$

$\omega_\mathbf{k} = \omega^{\pm}_\mathbf{k}(H = 0)$ and $\gamma_\mathbf{k} = 2\sum_\nu J_\nu \cos k_\nu$. The cross section was convoluted with the finite resolution function given by the Cooper and Nathans [17] approximation and then fitted to individual energy scans. This gave a good account of the observed scattering, and the resulting dispersion of the magnetic excitations is shown in Figs. 1(a)–1(c). The spin band along the c axis is more than 3 times wider than in the tetragonal plane. Adjusting Eq. (1) in a least-square fit, we find $\mu = 9.05(4)$ K, $s^2 J_{ab} = 0.16(1)$ K, and $s^2 J_c = 1.64(3)$ K, and, using Eqs. (3), we obtain $s^2 = 0.943$, $D = 8.12(4)$ K, $J_{ab} = 0.17(1)$ K, and $J_c = 1.74(3)$ K. The $S = 1$ spins of the Ni ions are thus strongly coupled along the tetragonal axis but only weakly perpendicular to it, making DTN a weakly coupled system of $S = 1$ chains with an anisotropy larger than the nearest-neighbor exchange interactions. The excellent description of the diagonal dispersion along the (h, h, h) direction using these parameters suggests that diagonal nearest-neighbor interactions are small.

Specific heat and the magnetocaloric effect (MCE) were measured in a dilution refrigerator system with an 18 T magnet at the National High Magnetic Field Laboratory in Los Alamos, New Mexico. All measurements were conducted on single crystals with the external field H oriented along the tetragonal c axis. Specific heat (100 mK $\leq T \leq$ 1.5 K) was determined by the quasiadiabatic heat pulse relaxation method, and the magnetocaloric effect was

measured by sweeping the field up and down at 0.01–0.05 T/min while monitoring the sample temperature with the bath temperature held fixed.

Distinct thermodynamic transitions can be observed in the specific heat and magnetocaloric effect data for H between 2.15 and 12.6 T. Representative data are shown in Figs. 2 and 3, and the phase diagram determined from these data is shown in Fig. 4. The specific heat data shown in Fig. 2 exhibit sharp peaks for $H = 3.5$ and 10 T. An equal entropy construction was used to determine the midpoint of the transition. For transitions occurring at a given temperature, the specific heat transition at high fields shows a taller peak than the transition at low fields. This asymmetry is due to the influence of the $S_z = -1$ excited state, which can play a role even at very low energies in this compound. The DTN compound is in a regime $2zJ/D \sim 1$ for which a two-level ($S_z = 1$ and $S_z = 0$) description does not work, and a more general theory for Bose-Einstein condensation incorporating all three levels is necessary [11].

In the magnetocaloric effect data shown in Fig. 3, heating is observed as the magnetic field is swept through the AF transition, surrounded by regions of cooling before and after the transition. The region of cooling after the transition can be attributed to a relaxation towards the bath temperature, and the cooling preceding the transition results from an increase in entropy of the spin systems at low temperatures as the $S_z = 1$ excited state approaches the ground state. The peak in the first derivative of $T(H)$, corresponding to maximum heating of the sample, was identified as the phase transition. The transition temperatures determined from specific heat and MCE are in excellent agreement as shown in Fig. 4. A second-order phase transition, such as the AF transition we are expecting in this compound, should exhibit heating when entering the ordered phase and cooling when leaving it. However, all of the MCE data show heating in both directions when the field is swept up and down. This may indicate a coupling to the lattice that results in an apparent first-order phase transition.

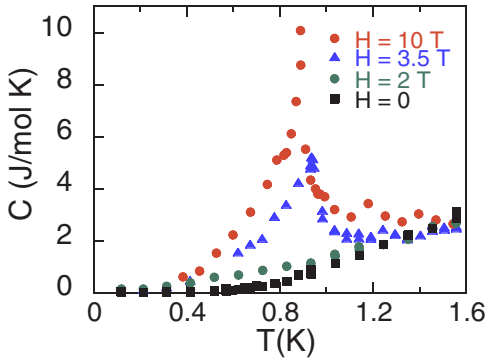

FIG. 2 (color online). Specific heat C versus temperature T of $NiCl_2$-4SC$(NH_2)_2$ for $H \| c$ in applied magnetic fields of 0, 2, 3.5, and 10 T.

The resulting phase diagram (Fig. 4) shows an ordered phase occurring between $H_{c1} \sim 2.1$ T and $H_{c2} \sim 12.6$ T with a maximum critical temperature of $T_c = 1.2$ K. The values of H_{c1} and H_{c2} extracted from this phase diagram are in agreement with those determined from magnetization to within a few percent [10]. The discrepancy could be due to slight orientation errors of the sample and the fact that, in the work by Paduan-Filho *et al.*, the onset of the transition is determined from the peak in the first derivative of $M(H)$, whereas a comparison with the midpoint of the transition in the specific heat and MCE effect would require taking the inflection point or the peak in the second derivative of $M(H)$. The values of the transition fields can be compared to theoretical predictions $g_c\mu_B H_{c1} = \sqrt{\mu^2 - 4s^2\mu\sum_\nu J_\nu}$ and $g_c\mu_B H_{c2} = D + 4\sum_\nu J_\nu$, using the quantities J and D determined from our neutron measurements, and $g_c = 2.26$ determined by susceptibility measurements [14]. The predicted value of the lower critical field $H_{c1} = 2.18(1)$ T is in very good agreement with the experimentally observed transitions. However, the predicted upper critical field $H_{c2} = 10.85$ T is somewhat smaller than the experimental value of 12.6 T from thermodynamic measurements. The discrepancy between theory and experiment is puzzling in light of the excellent agreement in H_{c1}. One possible explanation is a lattice distortion at high magnetic fields, which would lead to a change in the parameters D and J.

In order to study the occurrence of BEC of the Ni spins in DTN, we examine the temperature dependence of the AF phase boundary near H_{c1}. As mentioned before, a power-law temperature dependence $H_c(T) - H_{c1} \propto T^\alpha$, where $\alpha = 1.5$, is predicted for a transition to a BEC phase. In our fits to the $H_c(T)$ data for the compound DTN, we limit ourselves to investigating the low field side of the phase diagram due to the possibility of a magnetically induced strain phase occurring at high fields. The value of α is closely dependent on the value of H_{c1}, as well as on the temperature range of the fit. α is expected to approach 1.5 only as $T \to 0$. As a first step, we fix α and fit the $H_c(T)$ data to determine H_{c1}. This fit is performed for data between 100 mK and T_{max} and repeated for different trial values of α. The resultant H_{c1} as a function of T_{max} are

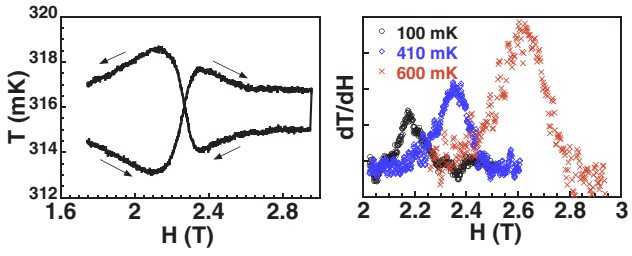

FIG. 3 (color online). Left: Magnetocaloric effect data determined by monitoring T while sweeping B up and down with a fixed bath temperature. Right: dT/dH for several temperatures, where the transition is identified as the peak.

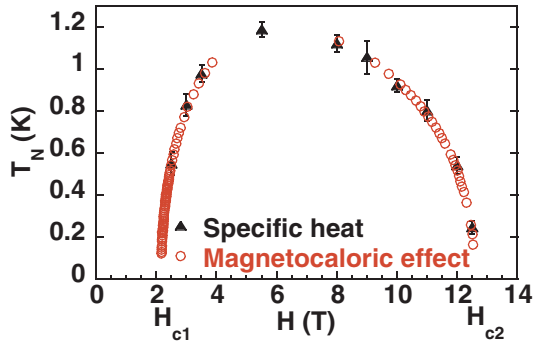

FIG. 4 (color online). Temperature T—magnetic field H phase diagram from specific heat and magnetocaloric effect data. Bose-Einstein condensation or canted AF order is thought to occur in the area under the symbols.

shown in Figs. 5(a) and 5(b). Two separate data sets were analyzed in this manner. Linear extrapolations of the low-temperature behavior of $H_{c1}(T_{\max})$ for different α converge very close to $T_{\max} = 0$, resulting in $H_{c1} = 2.149$ and 2.110 T for data sets 1 and 2, respectively. H_{c1} differs slightly for the two data sets due to small errors in centering of the sample in the magnetic field and alignment of the c axis (< 2 degrees). However, each data set is analyzed self-consistently so the exponent α is unaffected. In the expression $H_c(T) - H_{c1} \propto T^{\alpha}$, H_{c1} can now be fixed, and the phase diagram is fit to determine α as a function of $T_{\max}$ as shown in Figs. 5(c) and 5(d). $\alpha(T_{\max})$ is also determined for the lower and upper error bars of H_{c1}. Linear extrapolations to $T_{\max} = 0$ show that $\alpha(T_{\max} = 0)$ is consistent with the predicted value for 3D Bose-Einstein condensation of $\alpha = 1.5$ for both data sets and clearly inconsistent

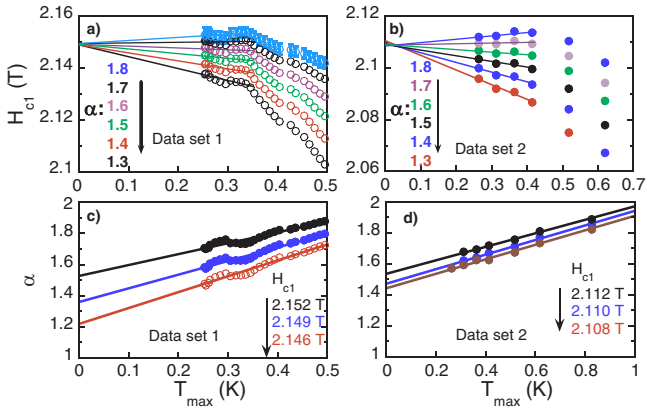

FIG. 5 (color online). Results from fits of two separate data sets by the expression $H_c(T) - H_{c1} \propto T^{\alpha}$ up to a maximum fit temperature $T_{\max}$ (see text). (a) and (b) show H_{c1} for various trials values of α. In (c) and (d), $\alpha(T_{\max})$ is determined using the value of H_{c1} found in (a) and (b). The upper and lower curves in (c) and (d) are determined using the upper and lower errors bars of H_{c1}.

prediction for a 2D BEC ($\alpha = 1$) or an Ising magnet ($\alpha = 2$). In summary, we have determined the spin Hamiltonian of DTN via inelastic neutron scattering, and we have mapped its high-field phase diagram using specific heat and magnetocaloric effect data. We show that DTN contains weakly coupled, tetragonally coordinated Ni^{2+} with a strong anisotropy and that the phase transition line near the QCP at H_{c1} is consistent with the BEC prediction $H_c(T) - H_{c1} \propto T^{\alpha}$, where $\alpha = 3/2$. Thus, DTN is the first quantum spin system containing Ni, rather than Cu dimers, to exhibit Bose-Einstein condensation of spin degrees of freedom.

This work was supported by the DOE, the NSF, and the Swiss National Science Foundation under Contract No. PP002-102831. A. P. F. acknowledges support from CNPq (Conselho Nacional de Desenvolvimento Científico e Tecnológico, Brazil). This work is partly based on experiments performed at the Swiss spallation neutron source SINQ, Paul Scherrer Institute, Villigen, Switzerland.

[1] Z. Honda, K. Katsumata, H. A. Katori, K. Yamada, T. Ohishi, T. Manabe, and M. Yamashita, J. Phys. Condens. Matter **9**, L83 (1997).
[2] N. Tateiwa, M. Hagiwara, H. Aruga-Katori, and T. C. Kobayashi, Physica (Amsterdam) **329B–333B**, 1209 (2003).
[3] H. Tsujii, Z. Honda, B. Andraka, K. Katsumata, and Y. Takano, Phys. Rev. B **71**, 014426 (2005).
[4] M. Jaime *et al.*, Phys. Rev. Lett. **93**, 087203 (2004).
[5] S. E. Sebastian, P. A. Sharma, M. Jaime, N. Harrison, V. Correa, L. Balicas, N. Kawashima, C. D. Batista, and I. R. Fisher, Phys. Rev. B **72**, 100404(R) (2005).
[6] C. Rüegg, N. Cavadini, A. Furrer, H.-U. Güdel, K. Krämer, H. Mutka, A. Wildes, K. Habicht, and P. Vorderwisch, Nature (London) **423**, 62 (2003).
[7] A. Oosawa, T. Takamasu, K. Tatani, H. Abe, N. Tsujii, O. Suzuki, H. Tanaka, G. Kido, and K. Kindo, Phys. Rev. B **66**, 104405 (2002).
[8] S. Sachdev, *Quantum Phase Transitions* (Cambridge University Press, Cambridge, England, 1999).
[9] V. N. Glazkov, A. I. Smirnov, H. Tanaka, and A. Oosawa, Phys. Rev. B **69**, 184410 (2004).
[10] A. Paduan-Filho, X. Gratens, and N. F. Oliveira, Phys. Rev. B **69**, 020405(R) (2004).
[11] H.-T. Wang and Y. Wang, Phys. Rev. B **71**, 104429 (2005).
[12] T. Nikuni, M. Oshikawa, A. Oosawa, and H. Tanaka, Phys. Rev. Lett. **84**, 5868 (2000).
[13] C. D. Batista (to be published).
[14] A. Paduan-Filho, R. D. Chirico, K. O. Joung, and R. L. Carlin, J. Chem. Phys. **74**, 4103 (1981).
[15] I. Affleck, Phys. Rev. B **43**, 3215 (1991).
[16] T. Giamarchi and A. M. Tsvelik, Phys. Rev. B **59**, 11 398 (1999).
[17] M. J. Cooper and R. Nathans, Acta Crystallogr. **23**, 357 (1967).